WASP-128b: a transiting brown dwarf in the dynamical-tide regime[*]

Vedad Hodžić[1][†], Amaury H. M. J. Triaud[1], David R. Anderson[2], François Bouchy[3], Andrew Collier Cameron[4], Laetitia Delrez[5], Michaël Gillon[6], Coel Hellier[2], Emmanuël Jehin[6], Monika Lendl[7,3], Pierre F. L. Maxted[2], Francesco Pepe[3], Don Pollacco[8], Didier Queloz[5,3], Damien Ségransan[3], Barry Smalley[2], Stéphane Udry[3], and Richard West[8]

[1]*School of Physics and Astronomy, University of Birmingham, Edgbaston, Birmingham B15 2TT, UK*
[2]*Astrophysics Group, Keele University, Staffordshire, ST5 5BG, UK*
[3]*Observatoire de Genève, Université de Genève, Chemin des Maillettes 51, 1290 Sauverny, Switzerland*
[4]*Centre for Exoplanet Science, SUPA School of Physics and Astronomy, University of St. Andrews, North Haugh, Fife, KY16 9SS, UK*
[5]*Cavendish Laboratory, J J Thomson Avenue, Cambridge, CB3 0HE, UK*
[6]*Institut d'Astrophysique et de Géophysique, Université de Liège, Allée du 6 Août, 17, Bat. B5C, Liège 1, Belgium*
[7]*Space Research Institute, Austrian Academy of Sciences, Schmiedlstr. 6, 8042 Graz, Austria*
[8]*Department of Physics, University of Warwick, Gibbet Hill Road, Coventry CV4 7AL, UK*

ABSTRACT

Massive companions in close orbits around G dwarfs are thought to undergo rapid orbital decay due to runaway tidal dissipation. We report here the discovery of WASP-128b, a brown dwarf discovered by the WASP survey transiting a G0V host on a 2.2 d orbit, where the measured stellar rotation rate places the companion in a regime where tidal interaction is dominated by dynamical tides. Under the assumption of dynamical equilibrium, we derive a value of the stellar tidal quality factor $\log Q'_\star = 6.96 \pm 0.19$. A combined analysis of ground-based photometry and high-resolution spectroscopy reveals a mass and radius of the host, $M_\star = 1.16 \pm 0.04\,M_\odot$, $R_\star = 1.16 \pm 0.02\,R_\odot$, and for the companion, $M_b = 37.5 \pm 0.8\,M_J$, $R_b = 0.94 \pm 0.02\,R_J$, placing WASP-128b in the driest parts of the brown dwarf desert, and suggesting a mild inflation for its age. We estimate a remaining lifetime for WASP-128b similar to that of some ultra-short period massive hot Jupiters, and note it may be a propitious candidate for measuring orbital decay and testing tidal theories.

Key words: methods: data analysis – brown dwarfs – binaries: eclipsing – planets and satellites: dynamical evolution and stability

1 INTRODUCTION

Brown dwarfs are substellar objects that occupy the mass range ~13–80 Jupiter masses, (MJ), thought to form via gravitational instability or molecular cloud fragmentation (Chabrier et al. 2014). Despite their abundance, however, very little is known about brown dwarfs. Most are found to be solitary, show complex spectral features that are difficult to model, and their masses are typically hard to estimate because the models are degenerate with their age, radius, and metallicity. Brown dwarf companions orbiting Sun-like stars offer a chance to study these objects in more detail as the stellar ages can be tied to the orbiting brown dwarf. Moreover, transit light curves can lift the inclination angle degeneracy to yield an unambiguous mass from radial velocity measurements, providing precise physical parameters that are crucial for testing substellar evolutionary models.

Despite being fully sensitive throughout the brown dwarf mass range, early Doppler surveys reported that brown dwarf companions are found in fewer numbers than their free-floating counterparts, termed the *brown dwarf desert* (Marcy & Butler 2000; Sahlmann et al. 2011;

---

[*] using data collected at ESO's La Silla Observatory, Chile: HARPS on the ESO 3.6m (Prog IDs 095.C-0105 & 097.C-0434), the Swiss *Euler* telescope, and TRAPPIST. The data is publicly available at CDS, and on demand to the main author.
[†] E-mail: vxh710@bham.ac.uk

Ma & Ge 2014). When comparing the same sample of host stars, up to 16 % of Sun-like stars have companions more massive than Jupiter, of which <1 % are brown dwarfs (Grether & Lineweaver 2006). Only twelve transiting brown dwarfs have been found to date (Bayliss et al. 2017 and references therein, Cañas et al. 2018), where just three have been detected from the ground, possibly due to a detection bias (Csizmadia et al. 2015). Only one other brown dwarf has been discovered by the WASP survey (WASP-30b; Anderson et al. 2011; Triaud et al. 2013).

Most massive substellar companions on close orbits have been found around F-type stars, and very few around G dwarfs, which has been interpreted as being due to rapid engulfment of massive planets and brown dwarfs around G dwarfs due to strong tidal coupling (Bouchy et al. 2011; Guillot et al. 2014; Damiani & Díaz 2016). Stars generally spin down as they age due to magnetic braking, where stellar winds carry highly ionised material that couples to the magnetic field lines and gets carried away from the star, leading to angular momentum loss. G dwarfs are typically more efficient at magnetic braking due to their deeper outer convective layer. However, companions on close orbits can transfer angular momentum from the orbit to the stellar spin, thereby draining angular momentum from the system via magnetic braking, leading to orbital decay until the companion is engulfed by the host. The rate of the companion's orbital decay is predicted to increase by up to three orders of magnitude in the dynamical-tide regime (Ogilvie & Lin 2007), with observational evidence on hot Jupiter hosts supporting stronger tidal coupling than for equilibrium tides (Collier Cameron & Jardine 2018). The strong dynamical tides from the companion excite inertial gravity waves (g-modes) in the convective layer that, in G dwarfs, break and dissipate in the radiative core, resulting in a spin-up the star from the inside (Barker & Ogilvie 2010; Essick & Weinberg 2016). Thus in systems where the host stars can be spun up by a massive companion such as a brown dwarf, the strong tidal coupling is expected to lead to runaway orbital decay of the companion onto the central star on short timescales compared to the lifetime of the star (Barker & Ogilvie 2010).

In this context we report the discovery of WASP-128b, a new transiting brown dwarf discovered by the WASP survey, orbiting a G0V host on a close orbit, where the measured stellar rotation rate places the system well-within the dynamical-tide regime, suggesting strong tidal coupling between the pair.

2 OBSERVATIONS

2.1 Photometry

WASP-128 is a moderately bright (V=12.5) G0V star at a distance of 422 ± 5 pc . The WASP survey (Pollacco et al. 2006) obtained 31 543 images of WASP-128 between 2006-05-04 and 2012-06-19, identifying a periodic 2.208 d transit signal in the photometry (Collier Cameron et al. 2006). Consequently, we initiated photometric and spectroscopic follow-up observations.

Five transits of WASP-128b were obtained using the 0.6 m TRAPPIST robotic telescope (Jehin et al. 2011; Gillon et al. 2011), located at ESO La Silla Observatory (Chile). The first of these transit observations is partial,

covering only the second half of the transit. All five transits were observed through a "blue-blocking" filter. The images are calibrated using standard procedures (bias, dark, and flat-field correction) and photometry is extracted using the IRAF/DAOPHOT[1] aperture photometry software (Stetson 1987), as described by Gillon et al. (2013). For each transit observation, a careful selection of both the photometric aperture size and stable comparison stars is performed manually to obtain the most accurate differential light curve of WASP-128. Some light curves are affected by a meridian flip; that is, the 180° rotation that TRAPPIST's equatorial mount has to undergo when the meridian is reached. We account for any potential photometric offset in our baseline model, see Section 3.2.

We observed three transits of WASP-128b using the EulerCam instrument installed at the 1.2 m *Euler* telescope also located at the La Silla site. The observations were carried out through an r'-Gunn filter and the telescope was slightly defocused to improve PSF sampling and observation efficiency. Each transit light curve is obtained using relative aperture photometry while optimizing reference star selection and extraction apertures to minimize the residual light curve RMS. The instrument and the associated data reduction is described in more detail in Lendl et al. (2012). Some of the images of WASP-128 leading up to and during the ingress of the second transit were saturated, and as such, we discarded a handful of observations in our analysis that had count levels above 50 000 ADU.

2.2 Spectroscopy

We collected 48 spectra from the CORALIE spectrograph on the *Euler* telescope between 2013-06-06 and 2016-11-24, as well as 23 HARPS spectra on the ESO 3.6 m telescope between 2015-04-02 and 2018-03-22. Both sets of data are reduced using similar data reduction softwares. Their resulting spectra are correlated with a numerical mask matching a G2V star (Baranne et al. 1996; Pepe et al. 2002). These procedures have been demonstrated to reach high precision and high accuracy (e.g. Mayor et al. 2009; López-Morales et al. 2014). We perform a single 3σ-clip on each radial velocity set using the line FWHM and bisector inverse slope span (BIS). One HARPS observation is discarded due to a highly discrepant BIS value, and one CORALIE observation was discarded due to the FWHM clip. Those outliers are highlighted in Appendix A.

3 DATA ANALYSIS

3.1 Spectral analysis

Using methods similar to those described by Doyle et al. (2013), we used the co-added HARPS spectrum to determine values for stellar effective temperature T_{eff}, surface gravity $\log g_\star$, metallicity [Fe/H], and projected stellar rotational

---

[1] IRAF is distributed by the National Optical Astronomy Observatory, which is operated by the Association of Universities for Research in Astronomy, Inc., under cooperative agreement with the National Science Foundation.

velocity $v \sin i_\star$. In determining $v \sin i$ we assumed a macro-turbulent velocity of 4.4 ± 0.7 km/s, based on the asteroseismic calibration of Doyle et al. (2014). Using MKCLASS (Gray & Corbally 2014) we obtain a spectral type G0V for WASP-128, which is consistent with the temperature derived from the spectral analysis. The Lithium abundance $\log A(\text{Li}) = 2.62 \pm 0.09$ suggests a relatively young age of 1–2 Gyr .

3.2 Global modelling

The combined data are analysed using `amelie`, a novel software package that jointly models the photometric and radial velocity data in a standard Bayesian framework. The code is essentially a Python wrapper on the `ellc` binary star light curve model (Maxted 2016) for computing exoplanet and eclipsing binary light curves and their radial velocity orbits, and the `emcee` affine-invariant Markov chain Monte Carlo (MCMC) sampler (Goodman & Weare 2010; Foreman-Mackey et al. 2013) for exploring the posterior parameter space.

We adopt a quadratic limb darkening law to model the intensity distribution of the stellar disc, using the `LDTk` package (Husser et al. 2013; Parviainen & Aigrain 2015) to sample band-specific limb darkening coefficients for the *Euler* and TRAPPIST datasets, following the triangular parametrisation described in Kipping (2013). No priors are imposed on the limb darkening parameters, rather, we fit the intensity profile of the disc using the built-in likelihood function, allowing uncertainties in the spectral parameters to be propagated to our final result. In addition, we sample the following parameters for our transit and radial velocity model: Period, P; mid-transit reference time, T_0; transit depth, D; transit width (time from first to fourth contact), W; impact parameter, b; and radial velocity semi-amplitude, K. Moreover, for our eccentric model we also sample the parameters $\sqrt{e} \sin \omega$ and $\sqrt{e} \cos \omega$, and in our orbital decay model we further sample $\dot{P} = dP/dt$. In all cases we use non-informative priors that are either physically bounded (e.g. $0 < b < 1$) or sensibly bounded to a wide enough region (e.g. $0 < K < 50 \, \text{km s}^{-1}$), where the transit midpoint is bounded by the light curves on 2014-03-03.

For each sampled set of parameters we further compute photometric and radial velocity baseline models. Our photometric baseline model consists of a normalisation factor with a second order polynomial in time for each light curve to allow for airmass and seeing effects. Moreover, we experimented with additional photometric detrending using sky background levels, FWHM changes in the PSF, and changes in the target pixel position on the CCD. Using the Bayesian Information Criterion (BIC; Schwarz 1978) to compare model complexity, we find that an additional first-order polynomial using sky background levels is strongly preferred for the *Euler* light curve on 2014-03-25. On the nights of 2014-02-11, 2014-03-03, and 2015-05-10, the TRAPPIST telescope peformed a meridian flip, for which we account for any potential offsets by allowing an additional normalisation factor before the flip. The radial velocity baseline model consists of a constant systemic velocity for each instrument. The CORALIE data is partitioned into two datasets due to an upgrade of the instrument that could affect the velocity zero-point (Triaud et al. 2017). We compare the constant velocity

model with models allowing a first- and second-order drift term, but find that any higher order terms are unjustified. The baseline model parameters are computed using a least-squares algorithm for every proposed parameter set in the MCMC sampling. Finally, we also sample additional errors on our photometry and radial velocity data to account for underestimated errors due to instrumental effects and stellar activity.

The mean stellar density can be estimated independently from a transit light curve and can be used with other observables to constrain the mass and age of a star from stellar evolution models (Seager & Mallén-Ornelas 2003; Triaud et al. 2013). We use BAGEMASS (Maxted et al. 2015) to estimate the age and mass of the host star, using our estimates of T_{eff} and [Fe/H] from the spectral modelling in Section 3.1, luminosity from *Gaia* DR2 (Andrae et al. 2018), and the mean stellar density from the transit light curves as inputs to the code. The mass is then used as input to our Keplerian model.

We initiate 256 walkers at positions normally dispersed close to the solution, and run each walker for 30 000 steps, chosen such that each walker is run for a few tens of autocorrelation lengths after discarding the first 15 000 steps as burn-in. The independent chains were thinned by a factor 100 due to autocorrelation, leaving each parameter with 38 400 independent samples, before computing the $\hat{R}$ statistic (Gelman et al. 2003), and mixing the chains. All parameters reach the recommended $\hat{R}<1.1$, indicating overall convergence.

4 RESULTS

Using BAGEMASS we find an age of $2.3 \pm 0.9 \, \text{Gyr}$ and mass of $M_\star = 1.16 \pm 0.04 \, M_\odot$ for WASP-128. From this we derive a radius of the star of $R_\star = 1.16 \pm 0.02 \, R_\odot$, and mass and radius of $M_b = 37.5 \pm 0.8 \, M_J$ and $R_b = 0.94 \pm 0.02 \, R_J$, for the companion, placing it securely in the brown dwarf regime. The best fit models with the photometric data are shown in Fig. 1, and in Fig. 2 for the radial velocity data. The results from our MCMC and derived parameters are shown in Table 1 with their 68 % confidence interval.

Eccentric model Given the close proximity to the host star, it is expected that the orbit of WASP-128b has been tidally circularised due to tidal dissipation in the brown dwarf as this would happen on a timescale of $\leq 1 \, \text{Gyr}$ (Barker & Ogilvie 2009). Nevertheless, when including eccentricity in our model, we derive a value of $e = 0.003^{+0.003}_{-0.002}$. Observational errors can lead to the detection of a small, non-zero, but spurious eccentricity (Lucy & Sweeney 1971). The BIC strongly disfavours an eccentric model compared to a circular fit. We apply the revised Lucy-Sweeney test (Lucy 2013) to put an upper limit of $e<0.007$ on the eccentricity using their uniform prior. The results of the other parameters between the two models are consistent with each other, and as such we present the results from the circular fit in Table 1, with our upper limit on the eccentricity.

Orbital decay model A periodic signal of $2.93 \pm 0.03 \, \text{d}$ was found in the photometric data (Maxted et al. 2011), which is consistent with the derived rotation period of
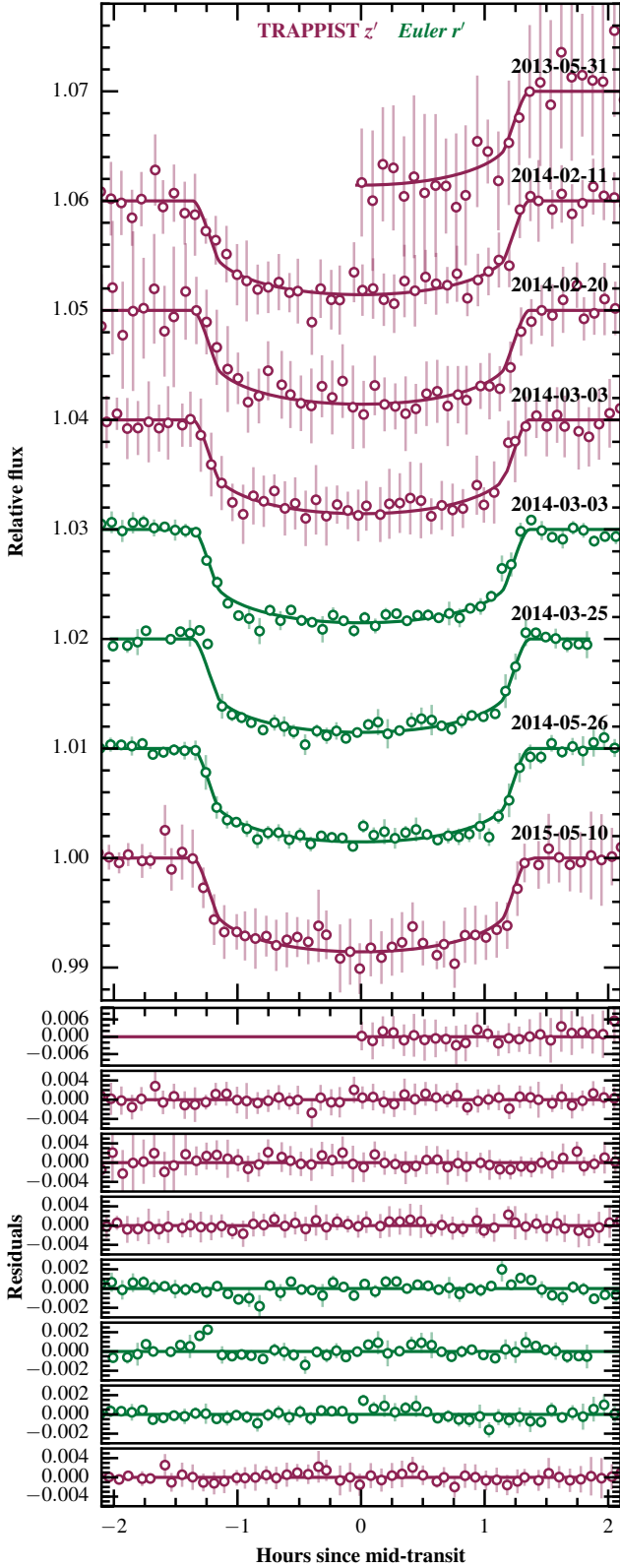
Figure 1. Transits of WASP-128 taken with the *Euler* (*green*) and TRAPPIST (*vermillion*) telescopes. The points correspond to detrended data binned to 5 minutes, and the coloured lines are the best fit models. The residuals of the fit are shown in the lower panel.
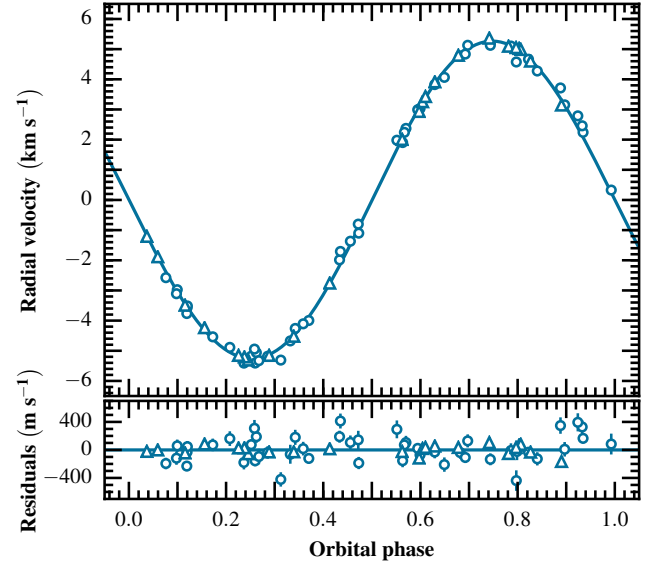
Figure 2. The radial velocity motion of WASP-128 due to its brown dwarf companion, folded on the best-fit period. The blue points correspond to RV measurements taken with CORALIE (*circles*) and HARPS (*triangles*). The solid line is the best-fit model. The residuals of the fit are shown in the lower panel.

Table 1. WASP128 system information and results. Numbers in brackets denote uncertainties on the last two digits the 16th and 84th percentiles. $\star$ and "b" subscripts denote the host star and companion, respectively.

Parameter	Value	Unit	Parameter	Value	Unit
		WASP-128			
		$11^{\mathrm{h}}31^{\mathrm{m}}26\overset{s}{.}10$ $-41°41'22\overset{''}{.}3$			
		2MASS J11312609-4141222			
		Gaia 5382697351745548416			
Spectral and system parameters					
T_{eff}	5950 ± 50	K	d	422 ± 6	pc
$\log g_\star$	4.1 ± 0.1	cgs	$\tau_\star$	2.2 ± 0.9	Gyr
[Fe/H]	0.01 ± 0.12	dex	G_{mag}	12.3	
$v \sin i_\star$	20.0 ± 1.2	km s^{-1}	Sp. type	G0V	
Sampled parameters					
P	$2.208524\left(^{+21}_{-20}\right)$	d	K	$5.272\left(^{+16}_{-16}\right)$	km s^{-1}
T_0	$2\,456\,720.68369\left(^{+19}_{-19}\right)$	BJD$_{\mathrm{UTC}}$	$q_1(r')$	$0.3679\left(^{+12}_{-12}\right)$	
D	$0.00699\left(^{+15}_{-15}\right)$		$q_2(r')$	$0.39437\left(^{+92}_{-92}\right)$	
W	$0.11290\left(^{+48}_{-44}\right)$	d	$q_1(z')$	$0.3805\left(^{+12}_{-12}\right)$	
b	$0.11\left(^{+10}_{-07}\right)$	$R_\star$	$q_2(z')$	$0.39827\left(^{+89}_{-89}\right)$	
Derived parameters					
$M_\star$	$1.155\left(^{+39}_{-39}\right)$	$M_\odot$	M_{b}	$37.19\left(^{+83}_{-85}\right)$	MJ
$R_\star$	$1.152\left(^{+21}_{-16}\right)$	$R_\odot$	R_{b}	$0.937\left(^{+22}_{-18}\right)$	RJ
$R_\star/a$	$0.1489\left(^{+24}_{-09}\right)$		R_{b}/a	$0.01246\left(^{+27}_{-18}\right)$	
$\rho_\star$	$0.807\left(^{+16}_{-38}\right)$	$\rho_\odot$	ρ_{b}	$55.9^{+2.6}_{-3.5}$	g cm^{-3}
$\log g_\star$	$4.396\left(^{+08}_{-08}\right)$	cgs	$\log g_{\mathrm{b}}$	$5.040\left(^{+13}_{-18}\right)$	cgs
a	$0.03590\left(^{+38}_{-40}\right)$	AU	i	$89.10\left(^{+63}_{-91}\right)$	°
$M_{\mathrm{b}}/M_\star$	$0.03074\left(^{+37}_{-35}\right)$		$f(m)$	$0.0000316\left(^{+03}_{-03}\right)$	$M_\odot$
$R_{\mathrm{b}}/R_\star$	$0.08359\left(^{+89}_{-88}\right)$		e	<0.007	
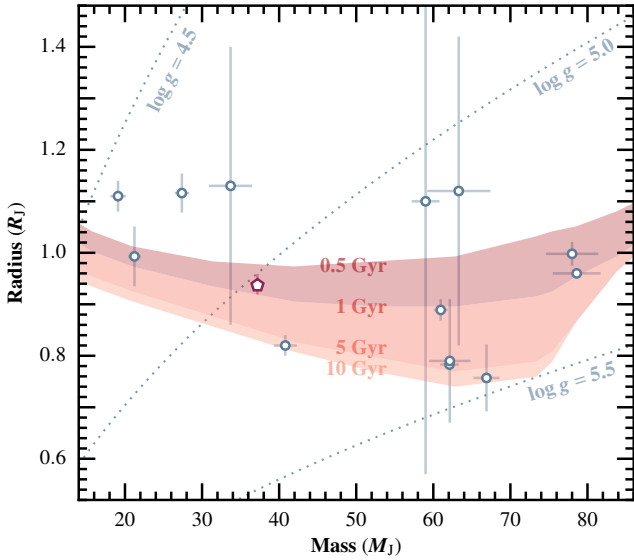
Figure 3. Mass-radius diagram placing WASP-128b (*vermillion*) in the context of the other known transiting brown dwarfs. Objects are from Bayliss et al. (2017) and references therein, including the recent discovery of Kepler-503b (Cañas et al. 2018). The shaded area outlines isochrones for substellar objects from the COND03 models (Baraffe et al. 2003).

$P_\star = 2.93 \pm 0.18$ d for WASP-128, using the observed $v \sin i_\star$ and $R_\star$. The fast rotation for an early G dwarf could indicate a tidal spin-up due to its massive companion. Given the expected strong tidal coupling in this system, we attempted to directly measure an orbital decay in the radial velocity data by including a period time-derivative, $\dot{P}$ in our model. We find that $\dot{P} = 1.05^{+1.13}_{-1.14}$ s year^{-1}, and note that, although not significant, we would not expect a positive $\dot{P}$ in our case where $P_{\rm orb} < P_\star$.

5 DISCUSSION

5.1 Tidal evolution

The orbital decay of the companion is significantly affected by magnetic braking as long as the total angular momentum of the system can remain above the critical limit (Damiani & Lanza 2015; Damiani & Díaz 2016),

$$L_{\rm crit} = 4 \left(\frac{G^2}{27} \frac{M_\star^3 M_{\rm b}^3}{M_\star + M_{\rm b}} (\beta(t) I_\star + I_{\rm b}) \right)^{\frac{1}{4}},$$

where $I = \alpha M R^2$ is the moment of inertia of the two objects, defined by their effective squared radii of gyration, α. The inclusion of $\beta(t)$ extends the original work by Hut (1980) to include the effects of orbital evolution due to magnetic braking, where $\beta = \Omega/n$ is the ratio of the stellar rotation rate to the orbital frequency, with $n^2 = G(M_\star + M_{\rm b})/a^3$. When $L > L_{\rm crit}$, the system can enter a pseudo-equilibrium state which is stable if the orbital angular momentum $L_{\rm orb}$ satisfies

$$L_{\rm orb} > (4 - \beta(t))(I_\star + I_{\rm b})n.$$

The companion satisfies both these criteria, so is thus either evolving towards the dynamically stable state, or is already

in synchronisation. Under the assumption of the latter, we can derive the stellar tidal dissipation parameter $Q'_\star$ that is needed to balance the tidal torque with the wind braking torque using relations in e.g. Brown et al. (2011) and Damiani & Díaz (2016), finding $\log Q'_\star = 6.96 \pm 0.19$. Recently, Collier Cameron & Jardine (2018) presented a study of the hot Jupiter population that yielded a value of $\log Q'_\star = 8.26 \pm 0.14$. In the regime where $0.5 < P/P_\star < 2$, dynamical tide become important (Ogilvie & Lin 2007). For a subset of hot Jupiters that fall into this range, the tidal dissipation parameter was found to be an order of magnitude smaller, where $\log Q'_\star = 7.31 \pm 0.39$, which is consistent with our estimate. In fact, using the above estimate for $Q'_\star$, we derive that the spin period of the star needed for a dynamically stable state is $2.80^{+0.44}_{-0.26}$ d, which increases confidence in our assumption about spin-orbit synchronisation. While in the dynamically stable state, the infall time of WASP-128b is given by the magnetic braking timescale, and we derive a remaining lifetime of 267^{+145}_{-67} Myr . In reality this is a lower limit, as the infall time will not be driven by magnetic braking once the companion is below the critical orbital period needed to stay in the dynamically stable state. Thereafter, the infall will proceed more slowly, but will still reach the Roche limit within a few tens of Myr (Fig. 3, Damiani & Díaz 2016).

More generally, lifetime estimates depend on the structural and rotational evolution of stars (Bolmont & Mathis 2016; Gallet et al. 2017). Using $\log Q'_\star = 6$ and implementing a dynamical model that includes tidal interactions between the star and companion, stellar evolution, magnetic braking, and tidal dissipation by gravity waves, Guillot et al. (2014) predicts a survival time of 50–60 % of the host's main-sequence lifetime for a companion at the mass of WASP-128b initially at a 3 d orbit. The main-sequence lifetime of WASP-128 with a mass of about $1.16\,M_\odot$ is ~6.9 Gyr , which corresponds to a lifetime of 3.5–4.2 Gyr for WASP-128b. The age estimated from BAGEMASS could thus be consistent with the companion's survival, although a thorough calculation of the companion's evolutionary history is needed to estimate its initial location (Brown et al. 2011).

5.2 Inflation

In Fig. 3 we place WASP-128b in a mass-radius diagram with the other known transiting brown dwarfs. WASP-128b sits in the driest part of the brown dwarf desert, $35 < m \sin i < 55\,M$J (Sahlmann et al. 2011; Ma & Ge 2014), coinciding with the ~$45\,M$J mass minimum found in Grether & Lineweaver (2006). It has been suggested that this minimum separates two brown dwarf populations differing by their formation mechanisms: The first formed in the protoplanetary disc via gravitational instability, and the second through molecular cloud fragmentation (Ma & Ge 2014). In this context, WASP-128b clearly belongs to the low-mass population of brown dwarfs.

Using our mass and age estimates for WASP-128b, the COND03 evolutionary models (Baraffe et al. 2003) predict a radius of $0.90\,R$J, which suggests a mild inflation compared to the measured radius. Irradiation effects should have little impact in inflating brown dwarfs, thus it is more likely due to some other mechanism that deposits energy in the brown dwarf interior (Bouchy et al. 2011).

6   CONCLUSION

We have discovered WASP-128b, a transiting brown dwarf from the WASP survey on a 2.2 d period around a G dwarf. Dynamical-tide theory predicts very few such objects should exist due to rapid orbital decay from strong stellar tidal coupling. Using radial velocity data collected over ~5 years, we rule out any significant orbital decay, and we derive a value of the stellar tidal quality factor based on an assumption of dynamical stability. The derived age, mass, and size of WASP-128b suggests a mild inflation, although we can not rule out a young age.

REFERENCES

Anderson D. R., et al., 2011, ApJ, 726, L19

Andrae R., et al., 2018, preprint, (arXiv:1804.09374)

Baraffe I., Chabrier G., Barman T. S., Allard F., Hauschildt P. H., 2003, A&A, 402, 701

Baranne A., et al., 1996, A&AS, 119, 373

Barker A. J., Ogilvie G. I., 2009, MNRAS, 395, 2268

Barker A. J., Ogilvie G. I., 2010, MNRAS, 404, 1849

Bayliss D., et al., 2017, AJ, 153, 15

Bolmont E., Mathis S., 2016, Celestial Mechanics and Dynamical Astronomy, 126, 275

Bouchy F., et al., 2011, A&A, 525, A68

Brown D. J. A., Collier Cameron A., Hall C., Hebb L., Smalley B., 2011, MNRAS, 415, 605

Cañas C. I., et al., 2018, preprint, (arXiv:1805.08820)

Chabrier G., Johansen A., Janson M., Rafikov R., 2014, Protostars and Planets VI, pp 619–642

Collier Cameron A., Jardine M., 2018, MNRAS, 476, 2542

Collier Cameron A., et al., 2006, MNRAS, 373, 799

Csizmadia S., et al., 2015, A&A, 584, A13

Damiani C., Díaz R. F., 2016, A&A, 589, A55

Damiani C., Lanza A. F., 2015, A&A, 574, A39

Doyle A. P., et al., 2013, MNRAS, 428, 3164

Doyle A. P., Davies G. R., Smalley B., Chaplin W. J., Elsworth Y., 2014, MNRAS, 444, 3592

Essick R., Weinberg N. N., 2016, The Astrophysical Journal, 816, 18

Foreman-Mackey D., Hogg D. W., Lang D., Goodman J., 2013, PASP, 125, 306

Gallet F., Bolmont E., Mathis S., Charbonnel C., Amard L., 2017, A&A, 604, A112

Gelman A., Carlin J., Stern H., Rubin D., 2003, Bayesian Data Analysis, Second Edition. Chapman & Hall/CRC Texts in Statistical Science, Taylor & Francis, https://books.google.co.uk/books?id=TNYhnkXQSjAC

Gillon M., Jehin E., Magain P., Chantry V., Hutsemékers D., Manfroid J., Queloz D., Udry S., 2011, in European Physical Journal Web of Conferences. p. 06002 (arXiv:1101.5807), doi:10.1051/epjconf/20101106002

Gillon M., et al., 2013, A&A, 552, A82

Goodman J., Weare J., 2010, Communications in Applied Mathematics and Computational Science, Vol.˜5, No.˜1, p.˜65-80, 2010, 5, 65

Gray R. O., Corbally C. J., 2014, AJ, 147, 80

Grether D., Lineweaver C. H., 2006, ApJ, 640, 1051

Guillot T., Lin D. N. C., Morel P., Havel M., Parmentier V., 2014, in EAS Publications Series. pp 327–336 (arXiv:1409.7477), doi:10.1051/eas/1465009

Hunter J. D., 2007, Computing In Science & Engineering, 9, 90

Husser T.-O., Wende-von Berg S., Dreizler S., Homeier D., Reiners A., Barman T., Hauschildt P. H., 2013, A&A, 553, A6

Hut P., 1980, A&A, 92, 167

Jehin E., et al., 2011, The Messenger, 145, 2

Jones E., Oliphant T., Peterson P., et al., 2001–, SciPy: Open source scientific tools for Python, http://www.scipy.org/

Kipping D. M., 2013, MNRAS, 435, 2152

Lendl M., et al., 2012, A&A, 544, A72

López-Morales M., et al., 2014, ApJ, 792, L31

Lucy L. B., 2013, A&A, 551, A47

Lucy L. B., Sweeney M. A., 1971, AJ, 76, 544

Ma B., Ge J., 2014, MNRAS, 439, 2781

Marcy G. W., Butler R. P., 2000, PASP, 112, 137

Maxted P. F. L., 2016, A&A, 591, A111

Maxted P. F. L., et al., 2011, Publications of the Astronomical Society of the Pacific, 123, 547

Maxted P. F. L., Serenelli A. M., Southworth J., 2015, A&A, 575, A36

Mayor M., et al., 2009, A&A, 493, 639

Ogilvie G. I., Lin D. N. C., 2007, ApJ, 661, 1180

Parviainen H., Aigrain S., 2015, Monthly Notices of the Royal Astronomical Society, 453, 3821

Pepe F., et al., 2002, The Messenger, 110, 9

Pollacco D. L., et al., 2006, PASP, 118, 1407

Sahlmann J., et al., 2011, A&A, 525, A95

Schwarz G., 1978, Annals of Statistics, 6, 461

Seager S., Mallén-Ornelas G., 2003, ApJ, 585, 1038

Stetson P. B., 1987, PASP, 99, 191

The Astropy Collaboration et al., 2018, preprint, (arXiv:1801.02634)

Triaud A. H. M. J., et al., 2013, A&A, 549, A18

Triaud A. H. M. J., et al., 2017, MNRAS, 467, 1714

Walt S. v. d., Colbert S. C., Varoquaux G., 2011, Computing in Science and Engg., 13, 22

Table A1. HARPS radial velocity dataset. Machine readable format is available online at CDS.
*marks data that was excluded from the fit.

BJD$_{UTC}$	RV km s^{-1}	σ km s^{-1}	FWHM km s^{-1}	BIS km s^{-1}
57114.60449	10.199	0.039	28.026	0.660
57114.76778	11.962	0.035	28.042	0.498
57115.58057	19.815	0.032	28.214	−0.434
57115.82146	17.866	0.034	28.531	−0.250
57116.70113	9.566	0.034	27.965	0.047
57135.56028*	19.322	0.042	28.009	−212.098
57137.58165	20.083	0.033	28.070	−0.144
57138.69441	9.412	0.038	27.943	−0.078
57139.64968	19.515	0.039	27.974	−0.005
57141.69566	17.976	0.033	28.064	−0.239
57157.59660	19.740	0.032	27.755	−0.305
57158.55661	9.516	0.029	27.901	−0.152
57181.51053	18.635	0.033	27.772	−0.243
57182.58397	11.229	0.035	27.986	−0.235
57183.57099	16.725	0.033	27.845	−0.148
57184.61904	13.512	0.040	28.024	0.015
57199.57186	19.709	0.042	27.545	−0.614
57202.55204	10.484	0.040	28.133	−0.408
57203.55602	18.147	0.041	27.747	−0.408
57204.54803	12.835	0.032	28.244	−0.435
57486.69800	19.769	0.035	27.994	−0.276
57487.64533	9.566	0.032	28.204	−0.330
58198.75802	9.995	0.033	27.887	0.242
58199.70887	17.653	0.030	27.825	0.085

Table A2. CORALIE (1) radial velocity dataset. Machine readable format is available online at CDS.
*marks data that was excluded from the fit.

BJD$_{UTC}$	RV km s^{-1}	σ km s^{-1}	FWHM km s^{-1}	BIS km s^{-1}
56449.55380	9.665	0.076	27.717	0.396
56684.77657	19.973	0.085	28.163	−0.189
56687.71939	12.270	0.082	27.557	−0.238
56690.80486	13.746	0.087	28.128	0.133
56692.78675	10.850	0.072	27.754	−0.019
56693.78537	19.512	0.071	27.966	−0.041
56694.75146	9.439	0.077	27.920	−0.203
56696.65091	11.269	0.080	28.071	−0.373
56697.70998	17.875	0.080	27.920	−0.315
56714.74762	9.537	0.103	27.634	−0.818
56718.73806	11.081	0.071	28.142	−0.279
56722.74814	17.087	0.075	28.026	−0.302
56726.60736	19.622	0.088	28.059	0.274
56739.66716	17.838	0.069	28.309	−0.371
56740.82885	11.331	0.081	28.037	0.181
56743.72944	12.860	0.085	27.873	−0.480
56748.71857	19.682	0.080	28.054	0.583
56773.54714	17.305	0.094	27.933	−0.508
56809.61602	9.787	0.087	27.887	−0.282
56810.57686	19.974	0.093	27.824	0.032
56811.62676	10.308	0.090	27.630	−0.422
56833.55362	11.871	0.090	27.655	−0.320
56837.52357	17.999	0.104	28.344	0.255
56878.47192	13.139	0.106	28.821	−0.025
56879.47225	18.559	0.117	27.563	0.278
56880.47542*	10.586	0.108	29.586	0.463

Table A3. CORALIE (2) radial velocity dataset. Machine readable format is available online at CDS.

BJD$_{UTC}$	RV km s^{-1}	σ km s^{-1}	FWHM km s^{-1}	BIS km s^{-1}
56998.82783	17.470	0.129	27.089	-0.397
57010.83242	10.576	0.098	28.247	-0.275
57015.84790	18.507	0.090	28.091	-0.496
57023.75181	9.795	0.105	28.255	0.046
57026.76127	17.054	0.095	27.886	-0.353
57068.72194	16.923	0.082	27.847	-0.233
57079.75804	16.586	0.093	27.882	-0.248
57081.72933	13.314	0.099	27.791	-0.205
57119.49079	16.662	0.127	27.879	-0.930
57121.52414	13.881	0.130	27.918	-0.248
57138.72284	9.737	0.120	28.154	-0.860
57188.50731	19.256	0.146	28.724	-0.472
57370.81271	10.009	0.135	28.450	0.138
57371.84319	19.658	0.124	28.396	-0.224
57422.73842	18.958	0.094	28.503	-0.362
57423.72168	9.500	0.089	27.995	-0.069
57458.64831	11.574	0.094	28.152	-0.403
57477.53671	18.747	0.102	28.080	0.084
57560.56102	9.273	0.099	28.367	0.085
57569.46427	9.354	0.111	28.101	0.128
57590.48972	19.784	0.103	27.711	0.100
57716.84880	15.010	0.149	27.543	-1.162

Table B1. Light curve information for WASP-128.

Date	Instrument	Filter	t_{exp} s	N	Baseline function
2013-05-31	TRAPPIST	Sloan z'	8	705	$p(t^2)$
2014-02-11	TRAPPIST	Sloan z'	11	832	$p(t^2) + MF$
2014-02-20	TRAPPIST	Sloan z'	11	1014	$p(t^2)$
2014-03-03	TRAPPIST	Sloan z'	11	860	$p(t^2)$
2014-03-03	*Euler*	Gunn r'	60	215	$p(t^2) + MF$
2014-03-25	*Euler*	Gunn r'	75	136	$p(t^2 + sky^1)$
2014-05-26	*Euler*	Gunn r'	60	203	$p(t^2)$
2015-05-10	TRAPPIST	Sloan z'	8	969	$p(t^2) + MF$

APPENDIX A: RADIAL VELOCITIES

APPENDIX B: PHOTOMETRIC INFORMATION

This paper has been typeset from a TeX/LaTeX file prepared by the author.